The British Journal of Radiology, 85 (2012), e837–e844

Differentiation of early hepatocellular carcinoma from benign hepatocellular nodules on gadoxetic acid-enhanced MRI

[1]H RHEE, MD, [1,2]M-J KIM, MD, PhD, [1,2]M-S PARK, MD, PhD and [1]K A KIM, MD

[1]*Department of Radiology, Yonsei University Severance Hospital, Seoul, Republic of Korea, and* [2]*Research Institute of Radiologic Science, Yonsei University Severance Hospital, Seoul, Republic of Korea*

Objective: To test new diagnostic criteria for the discrimination of early hepatocellular carcinoma (HCC) from benign hepatocellular nodules on gadoxetic acid-enhanced MRI (Gd-EOB-MRI).

Methods: We retrospectively analysed 34 patients with 29 surgically diagnosed early HCCs and 31 surgically diagnosed benign hepatocellular nodules. Two radiologists reviewed Gd-EOB-MRI, including diffusion-weighted imaging (DWI), and the signal intensity at each sequence, presence of arterial enhancement and washout were recorded. We composed new diagnostic criteria based on the lesion size and MRI findings, and then the diagnostic performance was compared with that of conventional imaging criteria with logistic regression and a generalised estimating equation method.

Results: A size cut-off value ($\geq$1.5 cm diameter) and MRI findings of T_1 hypointensity, T_2 hyperintensity, DWI hyperintensity on both low and high *b*-value images (b=50 and 800 s mm^{-2}, respectively), arterial enhancement, late washout and hepatobiliary hypointensity were selected as the diagnostic criteria. When lesions were considered malignant if they satisfied three or more of the above criteria, the sensitivity was significantly higher than when making a diagnosis based on arterial enhancement and washout alone (58.6% *vs* 13.8%, respectively; p=0.0002), while the specificity was 100.0% for both criteria.

Conclusion: Our new diagnostic criteria on Gd-EOB-MRI may help to improve the discrimination of early HCC from benign hepatocellular nodules.

Received 30 August 2011
Revised 21 November 2011
Accepted 24 January 2012

DOI: 10.1259/bjr/13212920

With surveillance programmes using ultrasound and serum α-fetoprotein assays for the diagnosis of hepatocellular carcinoma (HCC), HCCs can be diagnosed at an earlier stage, and this contributes to an improved prognosis [1]. As a result of advances in diagnostic examinations such as CT and MRI, vast numbers of small lesions can be identified in cirrhotic liver, and differentiation of HCC from benign hepatocellular nodules has emerged as an important problem in HCC surveillance [2].

Early HCC, a very well-differentiated HCC with a vaguely nodular appearance, is considered to correspond to a carcinoma *in situ* and is characterised by an indistinct margin without capsule formation, vascular invasion or intrahepatic metastasis [3, 4]. These lesions are often hypovascular and lack arterial enhancement or a washout pattern [5, 6]; thus, in dynamic contrast-enhanced studies, they may show similar imaging findings to those of benign hepatocellular nodules of cirrhotic liver, such as dysplastic nodules.

Gadoxetic acid disodium (Primovist®; Bayer Shering Pharma, Berlin, Germany), a new liver-specific contrast agent, recently became clinically available. Gadoxetic acid has the properties of an extracellular matrix agent that allows dynamic perfusion imaging, as well as a hepatocyte-specific agent that enables the evaluation of delayed hepatocyte uptake and excretion. Several previous studies have shown that, by combining the hepatobiliary phase and dynamic MRI, detection and characterisation of small HCCs are improved [7–11]. Detection of an early or well-differentiated HCC can be improved when it is depicted as a hypointense lesion on hepatobiliary phase images of gadoxetic acid-enhanced MRI (Gd-EOB-MRI) [8, 12]. However, benign hepatocellular lesions, such as dysplastic nodules, can also be seen as hypointense on hepatobiliary phase images, making them difficult to discriminate from HCC [13]. The purpose of our study was to test new diagnostic criteria for discrimination of early HCC from benign hepatocellular nodules on Gd-EOB-MRI through a retrospective analysis of surgically proven early HCC and benign hepatocellular nodules.

Methods and materials

Patients

This retrospective study was approved by the institutional review board at our institution, and the requirement for informed consent was waived. From January 2008 to December 2009, 345 consecutive patients underwent hepatectomy for HCC (n=264) or liver transplantation for liver cirrhosis or HCC (n=82) at our institution.

Address correspondence to: Dr Myeong-Jin Kim, Yonsei University Severance Hospital, 50 Yonsei-ro, Seodaemun-gu, Seoul 120-752, Republic of Korea. E-mail: kimnex@yuhs.ac

One patient underwent both hepatectomy and transplantation because of recurrent HCC after the hepatectomy. All surgical specimens were routinely sliced to 1 cm thickness and carefully inspected by pathologists. Conspicuous nodular lesions (large or discoloured ones), selected by the pathologists, were made into slides and microscopically examined. The final pathological diagnosis of early HCC was made by an experienced pathologist at our institution, who is a member of the International Consensus Group for Hepatocellular Neoplasia (ICGHN), using the latest pathological criteria of the ICGHN [3].

Of the 345 patients, 66 with pathologically identified early HCC or benign hepatocellular nodules on surgical specimens were eligible for this study. Among these 66 patients with 222 lesions, 162 lesions were excluded for the following reasons: (a) the patient did not undergo Gd-EOB-MRI on the 3 T system within 3 months before surgery at our institution (30 patients with 113 lesions) and (b) the location of the lesion described on the pathology report or photograph of the gross specimen could not be matched with MRI (49 lesions).

The remaining 34 patients with 60 surgically proven lesions (29 early HCCs, 9 high-grade dysplastic nodules, 8 low-grade dysplastic nodules, 12 large regenerative nodules and 2 focal nodular hyperplasia-like nodules) were included in our study. There were 30 male and 4 female patients, with a mean age of 57 years (range 30–66 years), and the diameter of the lesions ranged from 0.3 to 3.0 cm (mean 1.29 cm). The demographic and clinical characteristics of the patients are summarised in Table 1.

Imaging technique

All patients underwent preoperative MRI on a 3 T system (Magnetom® Trio Tim; Siemens, Erlangen, Germany). A 12-channel phased-array coil was used in all patients. The time interval between MRI and surgery was between 1 and 64 days (mean 17 days). All images were acquired in the transverse plane with the field of view ranging from 300 to 400 mm and a 75–80% rectangular field of view, depending on the patient's abdominal girth.

The MRI protocol consisted of pre-contrast and contrast-enhanced T_1 weighted imaging (T_1WI) obtained by a three-dimensional gradient echo sequence, T_2 weighted imaging (T_2WI) obtained by a fat-saturated fast spin echo sequence, diffusion-weighted imaging (DWI) obtained by respiratory-triggered, fat-suppressed single-shot echoplanar sequences (b-value=0, 50, 800 s mm^{-2}) and 20 min delayed hepatobiliary phase imaging obtained by the same sequence as used for dynamic imaging. The MRI sequences were obtained in the order listed. Pulse sequence parameters are listed in Table 2.

For contrast-enhanced dynamic MRI, 0.025 mmol kg^{-1} of body weight of gadoxetic acid disodium was injected at a rate of 2 ml s^{-1} as a rapid bolus and was immediately followed by a saline flush of 20 ml. A three-dimensional spoiled gradient-recalled echo sequence with chemically selective fat suppression was performed during suspended respiration at 30–35 s (arterial phase), 60–70 s (portal phase), 90–100 s (hepatic venous phase) and 120–150 s (equilibrium phase) after the intravenous injection of the contrast agent. Additional hepatobiliary phase images were obtained at 20 min after injection.

Image analysis

Two experienced radiologists (MSP, KAK) independently reviewed the pre-operative MRI. The two observers were informed of the lesion location by series/image number and arrows on the images from the picture archiving and communication system (PACS) but were blinded to the pathological diagnosis, clinical information and the original radiological report. Each reader recorded the signal intensities of the lesions on each sequence compared with the surrounding liver parenchyma, and the lesion was then categorised as hypo-, iso- or hyperintense. If a lesion was partially hypointense or hyperintense, it was categorised based on the dominant signal intensity. Arterial enhancement (defined as higher lesion intensity on the arterial phase than on pre-contrast T_1WI), washout (defined as hypointensity of the lesion compared with the surrounding liver parenchyma on late phase dynamic images—portal, hepatic venous or equilibrium phase) and hyperintensity

Table 1. Summary of the demographic and clinical characteristics of the patients

Parameter		*n* (%)
Sex	Male	30 (88.2)
	Female	4 (11.8)
Liver disease	Cirrhosis	33 (97.1)
	Chronic hepatitis	1 (2.9)
Aetiology of liver disease	Hepatitis B	28 (82.4)
	Hepatitis C	1 (2.9)
	Alcohol abuse	4 (11.8)
	Other	1 (2.9)
Child–Pugh class	Class A	28 (82.4)
	Class B	4 (11.8)
	Class C	2 (5.9)
Surgery	Hepatectomy for HCC	16 (47.1)
	Liver transplantation for HCC	17 (50.0)
	Liver transplantation for cirrhosis	1 (2.9)

HCC, hepatocellular carcinoma.

Table 2. Pulse sequence parameters for MRI

Parameter	Fat-suppressed T_2 weighted turbo spin echo	Gadoxetic acid-enhanced three-dimensional gradient echo	Respiratory-triggered diffusion-weighted echoplanar
Matrix	192×256	192×256	108×192
Section thickness (mm)	6	2	6
Intersection gap (mm)	1	–	1
Repetition time (ms)	2000	2.54	2000
Echo time (ms)	88	0.95	88
Flip angle (degrees)	150	13	150
Reduction factor	2	2	2

on DWI at both low and high *b*-value images (b=50, 800 s mm^{-2}, respectively) were also recorded to evaluate the sensitivity and specificity of each finding for the discrimination of early HCC and benign hepatocellular nodules [7, 13–17]. 2 weeks after the independent reviews, consensus opinions were obtained in conference.

Statistical analysis

The sizes of the benign hepatocellular nodules and early HCCs were compared using a linear mixed model, and an optimal cut-off value was determined using logistic regression with the generalised estimating equation (GEE) and Youden's index. The size cut-off value was used as one of the diagnostic criteria in the subsequent analysis. For each of the six MRI findings and the size criterion, sensitivity, specificity, positive predictive value and negative predictive value were calculated for the diagnosis of HCC.

We composed new combined criteria consisting of MRI findings and a size cut-off value for the differentiation of malignant and benign nodules. For comparison of diagnostic performance between the new combined criteria and conventional arterial enhancement and washout criteria [18], sensitivities and specificities were calculated, and differences in sensitivities and specificities were evaluated using the Wald test with the GEE. We calculated the percentage agreement for each MRI finding and the 95% confidence intervals (CIs) with an adjustment for the clustering effect, using logistic regression with the GEE. Statistical analysis was performed using commercial statistical software (SAS® v. 9.1.3; SAS Institute Inc., Cary, NC). For all statistical analyses, there was adjustment for the clustering effect, and a two-tailed p-value <0.05 was considered to indicate statistical significance.

Results

Diagnostic performance of MRI findings and size cut-off value

The mean diameter of early HCCs (1.44 cm; range 0.40–3.00 cm) was significantly (p=0.047) larger than that of benign hepatocellular nodules (1.15 cm; range 0.30–2.00 cm). The best size cut-off value for diagnosis of HCC was ≥1.5 cm (sensitivity 58.6%, specificity 87.1%; Figure 1).

Three MRI findings—namely, hypointensity on pre-contrast T_1WI (T_1 hypointensity), hyperintensity on T_2WI (T_2 hyperintensity) and hyperintensity on DWI—were not sensitive (20.7%, 20.7% and 13.8%, respectively) but were highly specific (100% for all; Figure 2; Table 3). The MRI finding of increased arterial enhancement was also not sensitive (31.0%) but was highly specific (96.8%). Washout on later dynamic phase images and hypointensity on hepatobiliary phase images were more sensitive (62.1% and 93.1%, respectively) but less specific (83.9% for both) than the above MRI findings (Figures 3 and 4).

Combination of criteria

Various combinations of six MRI findings (T_1 hypointensity, T_2 hyperintensity, DWI hyperintensity, arterial enhancement, washout, hepatobiliary hypointensity) and the best cut-off value of size were compiled to propose the best combination of diagnostic criteria (Table 4). Based on our findings, the best combination for the diagnosis of early HCC was positivity for three or more of the seven findings.

If a diagnosis of HCC was made when three or more findings were positive, the sensitivity and specificity were 58.6% and 100.0%, respectively. If a diagnosis of HCC was made based on arterial enhancement and washout alone, the sensitivity and specificity were 13.8%

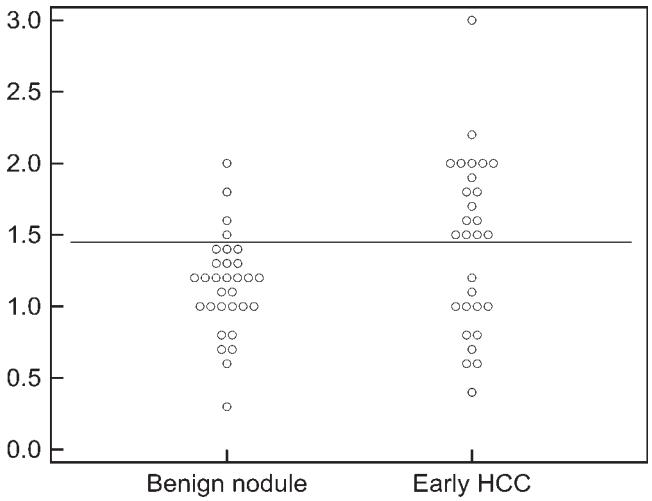

Figure 1. Size distributions of benign hepatocellular nodules and early hepatocellular carcinomas (HCCs). Early HCCs tend to be larger than benign hepatocellular nodules, with the best cut-off value of ≥1.5 cm (horizontal line).

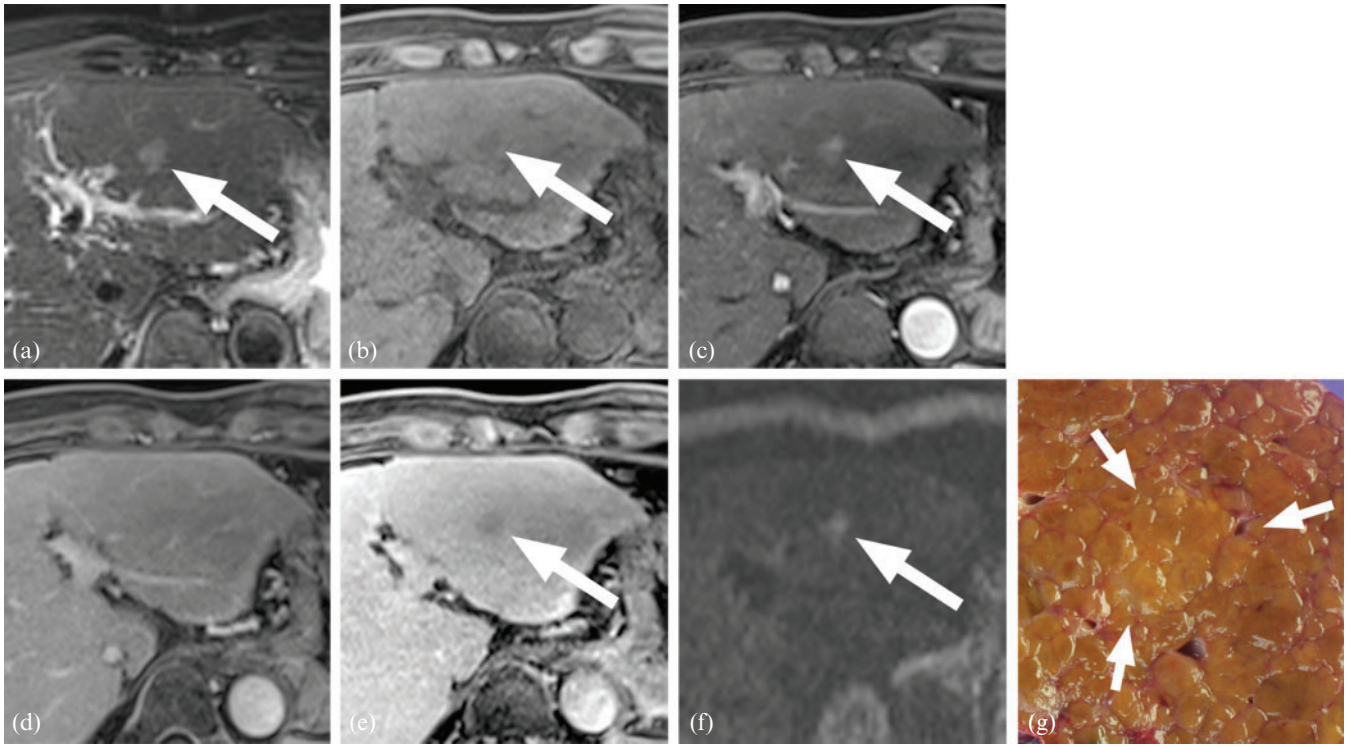

Figure 2. A 50-year-old male with a 1.5 cm early hepatocellular carcinoma: (a) T_2 weighted, (b) pre-contrast T_1 weighted, (c) arterial phase, (d) equilibrium phase, (e) hepatobiliary phase and (f) diffusion-weighted images (b=800 s mm^{-2}); (g) the gross specimen. The lesion showed hyperintensity on T_2 weighted imaging (a), hypointensity on T_1 weighted imaging (b), increased arterial enhancement (c), isointensity on portal phase images (d), hypointensity on hepatobiliary phase images (e), and hyperintensity on diffusion weighted images (f). This lesion satisfied six of the seven diagnostic criteria.

and 100.0%, respectively (Table 5). When only those lesions >1.0 cm were considered, the sensitivity and specificity of the new combined criteria (to diagnose HCC when three or more findings are positive) were 60.9% and 100.0%, respectively, compared with 13.0% and 100.0% with the conventional criteria of arterial enhancement and washout. The sensitivities of the new combined criteria were significantly higher than those of the conventional criteria for both data sets of all lesions (p=0.0002) and lesions >1.0 cm diameter (p=0.0006).

The percentage of agreement was >90% for all MRI findings (Table 6).

Discussion

Our results show that the new diagnostic criteria determined on Gd-EOB-MRI may improve the diagnostic sensitivity without compromising the specificity for the discrimination of early HCC from benign hepatocellular nodules. Specifically, the presence of three or more of the following findings in a hepatic nodule yields a sensitivity of 58.6% and specificity of 100%: T_1 hypointensity, T_2 hyperintensity, DWI hyperintensity, arterial enhancement, washout, hepatobiliary hypointensity and size ≥1.5 cm.

The imaging diagnosis of HCC based on increased arterial enhancement and decreased late phase enhancement has been the mainstay of non-invasive diagnosis of HCC in both the European Association for the Study of the Liver guidelines [19] and the American Association for the Study of Liver Disease guidelines [18]. Several recent studies have confirmed the high specificity of the conventional imaging criteria, even in small lesions (1–2 cm diameter); however, these studies also showed that false-negative findings were frequently seen in small or hypovascular HCCs [20–23]. In our study, early HCCs that are often hypovascular and usually <2 cm in diameter [24] showed low sensitivity (13.8%) using the conventional criteria, as was anticipated based on prior studies using CT [25, 26].

We evaluated six imaging findings on Gd-EOB-MRI and size for the differentiation of early HCC from benign hepatocellular nodules; none of these findings was acceptable as an isolated single finding. Therefore, we introduced new combined criteria that may be practically applicable. Our combined criteria showed a significant improvement in sensitivity compared with that of the arterial enhancement and washout criteria, while maintaining high specificity. The results of our study suggest that the addition of signal intensity evaluation of a lesion on T_1 weighted, T_2 weighted, diffusion-weighted and hepatobiliary phase images obtained using gadoxetic acid as a contrast agent and a size cut-off value can improve the sensitivity of diagnosis of early HCC, while maintaining a high specificity.

Several studies have reported that most well-differentiated HCCs show decreased hepatobiliary uptake on Gd-EOB-MRI [7, 12, 13]. In agreement with those reports, most early HCCs (93.1%) in this study showed hypointensity; by contrast, the majority of benign hepatocellular nodules (83.9%) showed iso- or

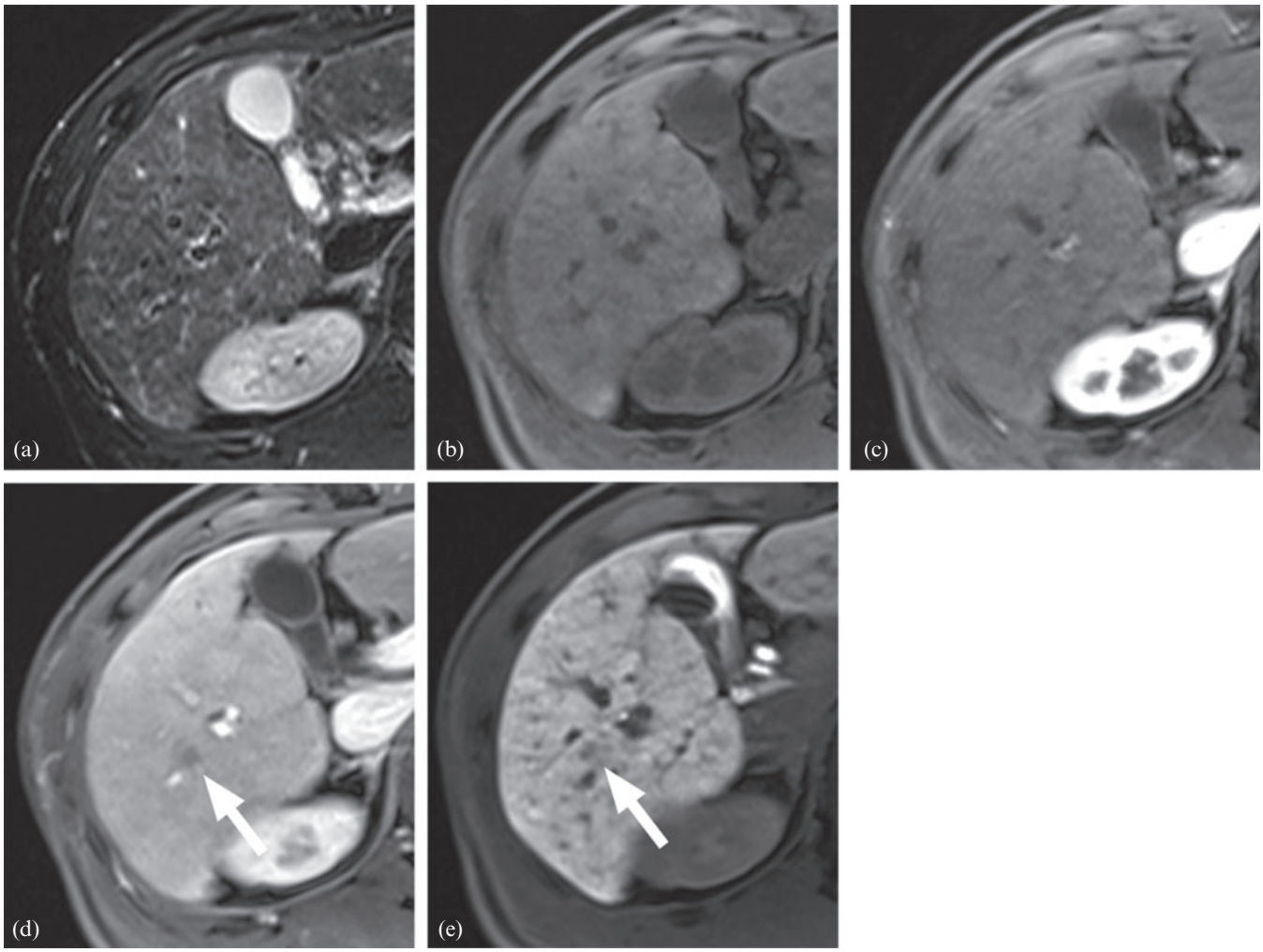

Figure 3. A 45-year-old male with a 1.0 cm early hepatocellular carcinoma (HCC): (a) T_2 weighted, (b) pre-contrast T_1 weighted, (c) arterial phase, (d) portal phase and (e) hepatobiliary phase images. The lesion was isointense on T_2 weighted imaging (a), pre-contrast T_1 weighted imaging (b) and arterial phase imaging (c). However, it showed decreased enhancement on portal phase (d) and hypointensity on hepatobiliary phase (e) images. The lesion satisfied two of seven criteria, which was insufficient for the diagnosis of HCC. However, the lesion was confirmed as early HCC after right lobectomy.

hyperintensity in the hepatobiliary phase. This suggests that even very well-differentiated HCCs have decreased hepatobiliary uptake, while most benign hepatocellular nodules do not. Hence, hypointensity in the hepatobiliary phase could be a useful predictor for differentiation between malignant and benign lesions. Nevertheless, there was considerable overlap in the hepatobiliary phases between the two groups. Quite a number of benign hepatocellular nodules (16.1%) showed hypointensity, as reported in other studies [9, 10, 13], and a small number of early HCCs showed iso- or hyperintensity in the hepatobiliary phase. Since hepatobiliary uptake primarily depends on expression of a molecular transporter, lesions with the same differentiation can show different hepatobiliary uptakes [27, 28]. Considering the overlap demonstrated in this study and the inherent limitation of hepatobiliary uptake, signal intensity in the hepatobiliary phase alone should be regarded as a useful finding for detection, rather than a finding for the diagnosis of HCC.

In our study, washout was defined as hypointensity in one of the later dynamic phase images, including portal, hepatic, venous and equilibrium phase images. Since the equilibrium phase is acquired approximately 120–150 s after the contrast injection, the decreased late phase enhancement is thought to reflect not only the rapid washout of contrast medium, but also early hepatobiliary uptake. Although the effect of early hepatobiliary uptake on the diagnostic performance of decreased late phase enhancement is not known, we can assume that hypointensity in late dynamic phase images might be reinforced by decreased hepatobiliary uptake.

Hyperintensity on DWI was used in our diagnostic criteria. Hyperintensity on DWI is known to suggest a malignant nature of nodular lesions, probably reflecting increased cellularity and vascular change [29], and, when combined with dynamic enhanced MRI, diagnostic performance can be improved [30, 31]. In our study, the sensitivity of hyperintensity on DWI in the diagnosis of early HCC was very low (13.8%); this might be related to less severe vascular change compared with that of progressed HCC [32], and a higher b-value (b=800 s mm^{-2}) in our study.

In our study, the size threshold of ≥1.5 cm was demonstrated to be useful for the discrimination of early

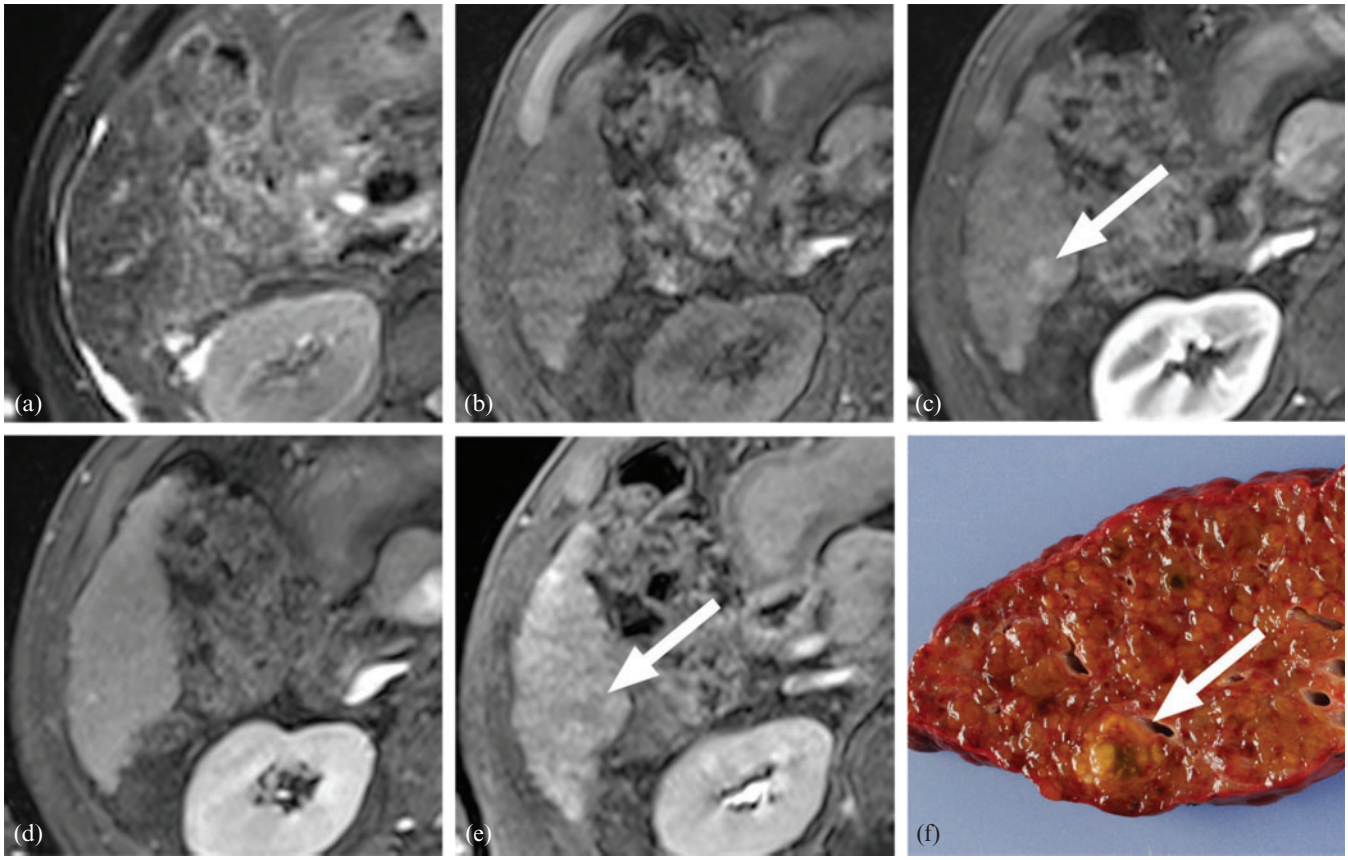

Figure 4. A 1.3 cm high-grade dysplastic nodule in a 66-year-old male: (a) T_2 weighted, (b) pre-contrast T_1 weighted, (c) arterial phase, (d) equilibrium phase and (e) hepatobiliary phase images; (f) the gross specimen. The lesion showed isointensity on T_2 weighted imaging (a) and pre-contrast T_1 weighted imaging (b). On dynamic imaging (c, d), slightly increased arterial enhancement was seen (c) without washout on the late phase images (d). Subtle hypointensity was noted in the lesion on hepatobiliary phase images (e). Two of the diagnostic criteria were met, rendering the diagnosis of a benign lesion.

HCC and benign hepatocellular nodules. This finding is concordant with results from previous studies showing that benign hepatocellular nodules in cirrhotic liver were usually <1.5 cm, and nodules ≥1.5 cm had a higher incidence of malignancy [21, 33, 34]. Hence, larger nodules should be considered as high-risk lesions, and a 1.5 cm size threshold might be a reasonable criterion.

Our study has several limitations. First, since this study is retrospective and included only surgically proven lesions, there might have been a potential selection bias. In the clinical setting, surgeons and pathologists are not blinded to the initial radiology report; lesions with a typical enhancement pattern or with many suspicious MRI findings are identified by careful inspection, and thus tend to be more frequently reported. Therefore, prospective evaluation will be necessary before our proposed criteria can be fully accepted. Second, most of the enrolled patients (28 patients with 48 lesions) were Child–Pugh Class A, well-compensated liver cirrhosis patients, and the remaining small number of patients (6 patients with 12 lesions) were Child–Pugh Class B or C. As the liver enhancement on hepatobiliary phase images may depend on liver function [35], it is uncertain whether the diagnostic performance of hepatobiliary phase images is lower in patients with advanced liver cirrhosis. Third, because there are

Table 3. Sensitivity, specificity, positive predictive value (PPV) and negative predictive value (NPV) of each finding

	Number of lesions				Diagnostic performance			
Finding	TP	FN	FP	TN	Sensitivity (%)	Specificity (%)	PPV (%)	NPV (%)
Arterial enhancement	9	20	1	30	31.0	96.8	90.0	60.0
Washout	18	11	5	26	62.1	83.9	78.3	70.3
T_1 hypointensity	6	23	0	31	20.7	100.0	100.0	57.4
T_2 hyperintensity	6	23	0	31	20.7	100.0	100.0	57.4
Hepatobiliary hypointensity	27	2	5	26	93.1	83.9	84.4	92.9
DWI hyperintensity	4	25	0	31	13.8	100.0	100.0	55.4
Nodule size ≥1.5 cm	17	12	4	27	58.6	87.1	81.0	69.2

DWI, diffusion-weighted imaging; FN, false negative; FP, false positive; TN, true negative; TP, true positive.

Table 4. Number of satisfied criteria and diagnostic performance

	Number of lesions				Diagnostic performance	
Number of satisfied criteria	TP	FN	FP	TN	Sensitivity (%)	Specificity (%)
1 or more	29	0	9	22	100.0	72.8
2 or more	25	4	6	25	86.2	82.2
3 or more	17	12	0	31	58.6	100.0
4 or more	7	22	0	31	24.1	100.0
5 or more	6	23	0	31	20.7	100.0
6	3	26	0	31	10.3	100.0

FN, false negative; FP, false positive; TN, true negative; TP, true positive.

Table 5. Sensitivity and specificity of conventional criteria and combined criteria

	All lesions		Lesions >1.0 cm in size	
Parameter	Sensitivity [% (CI)]	Specificity [% (CI)]	Sensitivity [% (CI)]	Specificity [% (CI)]
Arterial enhancement and washout	13.8 (5.1, 32.2)	100 (NA)	13.0 (4.1, 34.4)	100 (NA)
New diagnostic criteria[a] in our study	58.6 (39.4, 75.5)	100 (NA)	60.9 (40.3, 78.2)	100 (NA)
p-value	0.0002	NA	0.0006	NA

CI, confidence interval; NA, not applicable (95% CI and *p*-value could not be calculated owing to absence of false positives).
[a]Presence of three or more positive findings of T_1 hypointensity, T_2 hyperintensity, diffusion-weighted imaging hyperintensity, arterial enhancement, washout and hepatobiliary hypointensity, and size threshold $\geq$1.5 cm.

Table 6. Interobserver agreement

MRI findings	Reader 1 *vs* Reader 2 [percentage agreement (CI)]
Arterial enhancement	90.0 (78.1, 95.8)
Washout	90.0 (80.9, 95.0)
T_1 hypointensity	95.0 (85.3, 98.4)
T_2 hyperintensity	100.0 (NA)
Hepatobiliary hypointensity	96.7 (88.5, 99.1)
Diffusion-weighted imaging hyperintensity	93.3 (83.2, 97.5)

CI, confidence interval; NA, not applicable (95% CI could not be calculated because of 100% agreement between readers).

innumerable small nodular lesions in a cirrhotic liver, the possibility of misregistration between the surgical specimen and MRI cannot be excluded. Among these 66 patients with 222 lesions, 162 lesions were excluded for various reasons. The exclusion of this many lesions would be a significant limitation of the study. However, we carefully examined all available information (such as gross specimen photography, pathology reports, surgery notes) and excluded many lesions of uncertain location.

In conclusion, our study showed that the presence of three or more positive findings of T_1 hypointensity, T_2 hyperintensity, DWI hyperintensity, arterial enhancement, washout and hepatobiliary hypointensity, and the size threshold of $\geq$1.5 cm on Gd-EOB-MRI, may be sensitive and highly specific criteria for the discrimination of early HCC from benign hepatocellular nodules.

Acknowledgment

We would like to express our gratitude to Dr Young Nyun Park, for her thorough review of the pathological slides as well as for providing necessary information for completing this study.

References

1. Sangiovanni A, Del Ninno E, Fasani P, De Fazio C, Ronchi G, Romeo R, et al. Increased survival of cirrhotic patients with a hepatocellular carcinoma detected during surveillance. Gastroenterology 2004;126:1005–14.
2. Zech CJ, Reiser MF, Herrmann KA. Imaging of hepatocellular carcinoma by computed tomography and magnetic resonance imaging: state of the art. Dig Dis 2009;27:114–24.
3. International Consensus Group for Hepatocellular Neoplasia. Pathologic diagnosis of early hepatocellular carcinoma: a report of the International Consensus Group for Hepatocellular Neoplasia. Hepatology 2009;49:658–64.
4. Sakamoto M. Pathology of early hepatocellular carcinoma. Hepatol Res 2007;37(Suppl. 2):S135–8.
5. Takayasu K, Muramatsu Y, Mizuguchi Y, Moriyama N, Ojima H. Imaging of early hepatocellular carcinoma and adenomatous hyperplasia (dysplastic nodules) with dynamic CT and a combination of CT and angiography: experience with resected liver specimens. Intervirology 2004;47:199–208.
6. Li CS, Chen RC, Tu HY, Shih LS, Zhang TA, Lii JM, et al. Imaging well-differentiated hepatocellular carcinoma with dynamic triple-phase helical computed tomography. Br J Radiol 2006;79:659–65.
7. Kim SH, Lee J, Kim MJ, Jeon YH, Park Y, Choi D, et al. Gadoxetic acid-enhanced MRI versus triple-phase MDCT

for the preoperative detection of hepatocellular carcinoma. AJR Am J Roentgenol 2009;192:1675–81.
8. Ahn SS, Kim MJ, Lim JS, Hong HS, Chung YE, Choi JY. Added value of gadoxetic acid-enhanced hepatobiliary phase MR imaging in the diagnosis of hepatocellular carcinoma. Radiology 2010;255:459–66.
9. Sun HY, Lee JM, Shin CI, Lee DH, Moon SK, Kim KW, et al. Gadoxetic acid-enhanced magnetic resonance imaging for differentiating small hepatocellular carcinomas (< or = 2 cm in diameter) from arterial enhancing pseudolesions: special emphasis on hepatobiliary phase imaging. Invest Radiol 2010;45:96–103.
10. Motosugi U, Ichikawa T, Sou H, Sano K, Tominaga L, Muhi A, et al. Distinguishing hypervascular pseudolesions of the liver from hypervascular hepatocellular carcinomas with gadoxetic acid-enhanced MR imaging. Radiology 2010;256: 151–8.
11. Di Martino M, Marin D, Guerrisi A, Baski M, Galati F, Rossi M, et al. Intraindividual comparison of gadoxetate disodium-enhanced MR imaging and 64-section multidetector CT in the detection of hepatocellular carcinoma in patients with cirrhosis. Radiology 2010;256:806–16.
12. Kawada N, Ohkawa K, Tanaka S, Matsunaga T, Uehara H, Ioka T, et al. Improved diagnosis of well-differentiated hepatocellular carcinoma with gadolinium ethoxybenzyl diethylene triamine pentaacetic acid-enhanced magnetic resonance imaging and Sonazoid contrast-enhanced ultrasonography. Hepatol Res 2010;40:930–6.
13. Kogita S, Imai Y, Okada M, Kim T, Onishi H, Takamura M, et al. Gd-EOB-DTPA-enhanced magnetic resonance images of hepatocellular carcinoma: correlation with histological grading and portal blood flow. Eur Radiol 2010;20:2405–13.
14. Kelekis NL, Semelka RC, Worawattanakul S, de Lange EE, Ascher SM, Ahn IO, et al. Hepatocellular carcinoma in North America: a multiinstitutional study of appearance on *T*1-weighted, *T*2-weighted, and serial gadolinium-enhanced gradient-echo images. AJR Am J Roentgenol 1998;170: 1005–13.
15. Willatt JM, Hussain HK, Adusumilli S, Marrero JA. MR imaging of hepatocellular carcinoma in the cirrhotic liver: challenges and controversies. Radiology 2008;247:311–30.
16. Xu PJ, Yan FH, Wang JH, Shan Y, Ji Y, Chen CZ. Contribution of diffusion-weighted magnetic resonance imaging in the characterization of hepatocellular carcinomas and dysplastic nodules in cirrhotic liver. J Comput Assist Tomogr 2010;34:506–12.
17. Hammerstingl R, Huppertz A, Breuer J, Balzer T, Blakeborough A, Carter R, et al. Diagnostic efficacy of gadoxetic acid (Primovist)-enhanced MRI and spiral CT for a therapeutic strategy: comparison with intraoperative and histopathologic findings in focal liver lesions. Eur Radiol 2008;18:457–67.
18. Bruix J, Sherman M. Management of hepatocellular carcinoma: an update. Hepatology 2011;53:1020–2.
19. Bruix J, Sherman M, Llovet JM, Beaugrand M, Lencioni R, Burroughs AK, et al. Clinical management of hepatocellular carcinoma. Conclusions of the Barcelona-2000 EASL conference. European Association for the Study of the Liver. J Hepatol 2001;35:421–30.
20. Bolondi L, Gaiani S, Celli N, Golfieri R, Grigioni WF, Leoni S, et al. Characterization of small nodules in cirrhosis by assessment of vascularity: the problem of hypovascular hepatocellular carcinoma. Hepatology 2005;42:27–34.
21. Forner A, Vilana R, Ayuso C, Bianchi L, Sole M, Ayuso JR, et al. Diagnosis of hepatic nodules 20 mm or smaller in cirrhosis: prospective validation of the noninvasive diagnostic criteria for hepatocellular carcinoma. Hepatology 2008;47:97–104.
22. Leoni S, Piscaglia F, Golfieri R, Camaggi V, Vidili G, Pini P, et al. The impact of vascular and nonvascular findings on the noninvasive diagnosis of small hepatocellular carcinoma based on the EASL and AASLD criteria. Am J Gastroenterol 2010;105:599–609.
23. Sangiovanni A, Manini MA, Iavarone M, Romeo R, Forzenigo LV, Fraquelli M, et al. The diagnostic and economic impact of contrast imaging techniques in the diagnosis of small hepatocellular carcinoma in cirrhosis. Gut 2010;59:638–44.
24. Kojiro M. Diagnostic discrepancy of early hepatocellular carcinoma between Japan and West. Hepatol Res 2007;37 (Suppl. 2):S121–4.
25. Takayasu K, Furukawa H, Wakao F, Muramatsu Y, Abe H, Terauchi T, et al. CT diagnosis of early hepatocellular carcinoma: sensitivity, findings, and CT-pathologic correlation. AJR Am J Roentgenol 1995;164:885–90.
26. Lee J, Lee WJ, Lim HK, Lim JH, Choi N, Park MH, et al. Early hepatocellular carcinoma: three-phase helical CT features of 16 patients. Korean J Radiol 2008;9:325–32.
27. Kitao A, Zen Y, Matsui O, Gabata T, Kobayashi S, Koda W, et al. Hepatocellular carcinoma: signal intensity at gadoxetic acid-enhanced MR imaging: correlation with molecular transporters and histopathologic features. Radiology 2010;256: 817–26.
28. Tsuboyama T, Onishi H, Kim T, Akita H, Hori M, Tatsumi M, et al. Hepatocellular carcinoma: hepatocyte-selective enhancement at gadoxetic acid-enhanced MR imaging: correlation with expression of sinusoidal and canalicular transporters and bile accumulation. Radiology 2010;255: 824–33.
29. Vandecaveye V, De Keyzer F, Verslype C, Op de Beeck K, Komuta M, Topal B, et al. Diffusion-weighted MRI provides additional value to conventional dynamic contrast-enhanced MRI for detection of hepatocellular carcinoma. Eur Radiol 2009;19:2456–66.
30. Xu PJ, Yan FH, Wang JH, Lin J, Ji Y. Added value of breathhold diffusion-weighted MRI in detection of small hepatocellular carcinoma lesions compared with dynamic contrast-enhanced MRI alone using receiver operating characteristic curve analysis. J Magn Reson Imaging 2009;29: 341–9.
31. Piana G, Trinquart L, Meskine N, Barrau V, Beers BV, Vilgrain V. New MR imaging criteria with a diffusion-weighted sequence for the diagnosis of hepatocellular carcinoma in chronic liver diseases. J Hepatol 2011;55: 126–32.
32. Park YN. Update on precursor and early lesions of hepatocellular carcinomas. Arch Pathol Lab Med 2011;135: 704–15.
33. Sakamoto M, Hirohashi S. Natural history and prognosis of adenomatous hyperplasia and early hepatocellular carcinoma: multi-institutional analysis of 53 nodules followed up for more than 6 months and 141 patients with single early hepatocellular carcinoma treated by surgical resection or percutaneous ethanol injection. Jpn J Clin Oncol 1998;28:604–8.
34. Bennett GL, Krinsky GA, Abitbol RJ, Kim SY, Theise ND, Teperman LW. Sonographic detection of hepatocellular carcinoma and dysplastic nodules in cirrhosis: correlation of pretransplantation sonography and liver explant pathology in 200 patients. AJR Am J Roentgenol 2002;179:75–80.
35. Motosugi U, Ichikawa T, Sou H, Sano K, Tominaga L, Kitamura T, et al. Liver parenchymal enhancement of hepatocyte-phase images in Gd-EOB-DTPA-enhanced MR imaging: which biological markers of the liver function affect the enhancement? J Magn Reson Imaging 2009;30: 1042–6.